

Direct observation of Dirac interface states at the $\text{Bi}_2\text{Se}_3/\text{Si}(111)$ interface

M. H. Berntsen, O. Götberg, and O. Tjernberg*

Materials Physics, KTH Royal Institute of Technology, S-16440 Kista, Sweden

(Dated: November 5, 2018)

Topological insulators with mass-less helical Dirac fermions on their surface have attracted considerable attention in recent years. Several exotic effects and proposed applications rely on the presence of such states also at the interface between a topological insulator and a trivial insulator. In the present work, we have used low-energy angle-resolved photoelectron spectroscopy to demonstrate and characterize the interface states at the substrate interface in Bi_2Se_3 thin films grown on $\text{Si}(111)$. The results establish that Dirac fermions are indeed present also at the interface. It is also shown that the interface states are shifted in energy with respect to the surface states due to band bending in the film. The observation of topological interface states paves the way for further studies of interface related phenomena involving topological insulator thin films.

The three-dimensional (3D) topological insulators (TIs) constitute a class of materials in which the inverted band structure of the insulating bulk is accompanied by the existence of conducting metallic states at the surface [1–3]. These surface states consist of massless helical Dirac fermions which are protected by time reversal symmetry and therefore robust against non-magnetic backscattering. Although discovered only recently, the TIs have been the subject of extensive research, not only due to their inherently interesting properties and potential impact on the development of room-temperature spintronic devices [4, 5] but also because they are predicted to make the realization of a number of exotic physical phenomena, such as Dyons [6], Majorana fermions [7] and axion dynamics [8], feasible. The binary compound Bi_2Se_3 , considered to be the model system for the 3D TI material class [9], has received a lot of attention in this context. Photoemission studies of single crystal Bi_2Se_3 have confirmed the nearly linear dispersion of the Dirac fermions [10] while the helicity has been investigated by recent spin-resolved measurements [11, 12].

Pioneering works on Bi_2Se_3 thin films have revealed a strong variation in the electronic band structure of the surface state as a function of film thickness [13]. At thicknesses below 5 quintuple layers (QL), one QL is 9.5 Å thick, an energy gap opens at the Dirac point as a result of hybridization between Dirac states originating from opposite sides of the film. The strength of the hybridization decreases rapidly with increasing film thickness and for 6 QL films it is negligible and the energy gap at the Dirac point closes. Experimental observations of this gap opening in ultra thin films provide indirect evidence for the existence of a Dirac state at the interface towards the substrate. In fact, theory predicts the existence of gapless topological Dirac states at interfaces between topologically trivial materials and TIs [14]. Consequently, such states should exist at the interface between a TI thin film and the substrate on which it is grown. However, so far

no direct observation of buried-interface states in non-hybridized TI films has been made. It is therefore, first of all, of fundamental interest to experimentally establish the existence of interface states in a TI-semiconductor junction. Additionally, a qualitative description of how the electron configuration in thin films is influenced by the presence of the substrate, including a band alignment model for the junction, is desirable, something which thus far has only been discussed briefly [15–17]. Once understood, the latter can provide insights on how to tailor the electronic properties, e.g. the position of the chemical potential, of a TI film by changing properties of the substrate. Such tailoring can prove useful not only in future realization of some of the mentioned exotic phenomena but also for practical device applications. In this Letter we address these issues and provide experimental evidence for the existence of Dirac fermions at the substrate interface in thin films and show how the band bending through the film can be explained by band alignment between the film and the substrate at the interface.

In the present work we have studied the electronic band structure of Bi_2Se_3 thin films by means of laser-based Angle-Resolved Photoelectron Spectroscopy (ARPES). In order to enable direct observation of the buried-interface state a combination of low photon energy and cryogenic sample temperature was used in the experiments since this dramatically increases the escape depth of the photoexcited electrons [18]. The photoemission experiments were performed at the BALTAZAR laser-ARPES facility [19] at a photon energy of 10.5 eV. Thin films of thicknesses 6 QL and 8 QL were grown *in situ* following the method described in Ref. [13], in which thin films are deposited by co-evaporation of Bi and Se onto a Bi-terminated $\text{Si}(111)-(7 \times 7)$ substrate. The specific film thicknesses were chosen so that hybridization between interface and surface Dirac states is avoided while, at the same time, the films are sufficiently thin for the interface to be directly probed by the ARPES experiment.

Figure 1 presents photoemission data of the 8 QL and 6 QL Bi_2Se_3 films. Both samples were grown on *n*-type

* oscar@kth.se

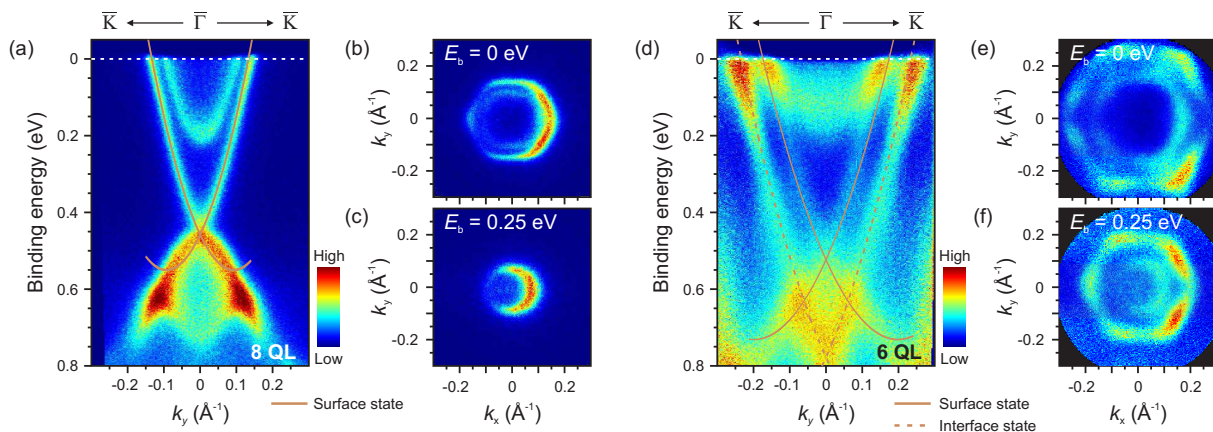


FIG. 1. (color online) (a)-(c) Photoemission intensity plots (raw data) of a 8 QL thick Bi_2Se_3 film on n -type Si-substrate taken at $h\nu = 10.5$ eV and $T = 9$ K. (a) Energy dispersion along the \bar{K} - $\bar{\Gamma}$ - \bar{K} direction. The fitted band structure described by Eq. 1 is plotted as solid lines on top of the experimental data. (b) Constant energy cut at E_F displaying the hexagonal Fermi surface. (c) Constant energy cut at $E_b=0.25$ eV. (d)-(f) Photoemission data of a 6 QL Bi_2Se_3 film on n -type Si-substrate taken at $h\nu= 10.5$ eV and $T = 9$ K. All energy distribution curves (EDCs) in the data set are normalized to unity in order to increase visibility of the interface state. (d) Measured energy dispersion along the \bar{K} - $\bar{\Gamma}$ - \bar{K} direction together with the fitted band structure of Eq. 2. Solid and dashed lines represent the surface and interface states, respectively. (e) Constant energy cut at E_F . Two hexagonal energy contours are observed, the inner one belonging to the surface state and the outer to the interface state. (f) Constant energy cut at $E_b = 0.25$ eV. The black areas in (e) and (f) are outside the detector, which explains why there are no counts in these areas.

doped (0.004 Ωcm) Si(111) substrates and the data were taken at $T = 9$ K. The energy-momentum slice for the 8 QL film, displayed in Fig. 1(a), shows a nearly linearly dispersing Dirac surface state with the Dirac point located at a binding energy (E_b) of 0.46 eV. As revealed by the constant energy cut taken at the Fermi level (E_F), shown in Fig. 1(b), the Fermi surface (FS) is hexagonally deformed. Closer to the Dirac point the constant energy surface becomes circular, as seen in Fig. 1(c). This deviation from an ideal Dirac cone has been reported previously [20] and is expected for highly n -doped Bi_2Se_3 samples. By using the single band model [21] described by

$$E_{\pm}(k) = E_0 - Dk^2 \pm \sqrt{\left(\frac{\Delta}{2} - Bk^2\right)^2 + (v_F \hbar k)^2}, \quad (1)$$

together with peak positions of momentum-distribution curves (MDCs) extracted from our data, we can create a fitted curve of the surface state. Here, E_{\pm} represent the dispersion of the Dirac state above and below the Dirac point respectively, E_0 is the binding energy of the Dirac point, Δ is the energy gap at the Dirac point (non-zero only if inter-surface coupling is present), v_F is the Fermi velocity and k the in-plane electron momentum. B and D are model parameters and their definitions are found in Ref. [21]. The resulting fitted curve is plotted on top of the experimental data in Fig. 1(a) (solid line) and the fitted model parameters are listed in Table 1. The model described by Eq. (1) is derived from an effective Hamiltonian and fits well with the data for small k -values. However, it does not include the hexag-

onal distortion of the Dirac cone. Therefore, only points in the region where no distortion of the cone is observed are included in the fit. Consequently, the resulting Fermi velocities (v_F) from the fits, listed in Table I, are smaller than reported elsewhere [15, 16]. For comparison, actual values of v_F are also given in Table I.

Comparing the energy-momentum slices in Figs. 1(a) and 1(d) for the 8 QL and 6 QL films respectively, reveals the presence of similar Dirac-like states in both films with the Dirac points located at nearly the same binding energies. However, in the 6 QL data there is an additional, much larger, V-shaped feature reminiscent of a Dirac state shifted towards higher binding energy. The constant-energy slice displayed in Fig. 1(e) is taken at E_F and shows that both of these features are hexagonally deformed similar to what we observe in the 8 QL film. For a constant-energy cut at higher binding energy the inner feature becomes circular, as seen in Fig. 1(f), since we are now approaching the Dirac point of this state, while the outer constant-energy surface remains hexagonal. The model fitted to the 8 QL data describes a single Dirac state only. Therefore, in order to determine the origin of the additional spectral feature seen in the 6 QL case we adopt the double band model from Ref. [17]. This model includes Dirac cones on opposite sides of the TI film and accounts for the structure inversion asymmetry (SIA) and the effective band bending induced by the presence of the substrate. The dispersion of the Dirac

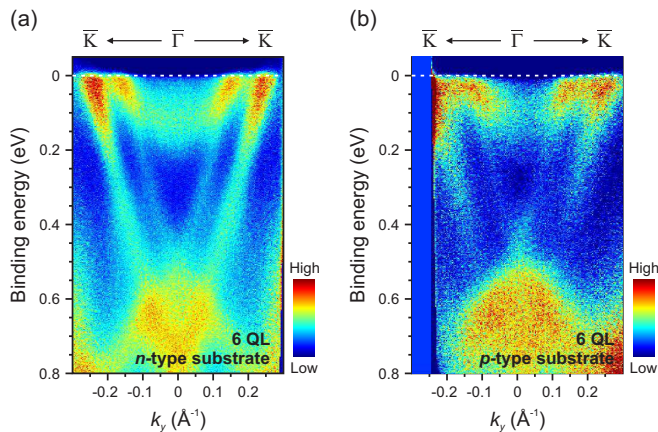


FIG. 2. (color online) (a) Energy dispersion along the $\bar{K}\text{-}\bar{\Gamma}\text{-}\bar{K}$ direction for a 6 QL Bi_2Se_3 grown on a n -type substrate. (b) Corresponding energy-momentum slice for a 6 QL film on p -type substrate. Due to missing data for k_y values below -0.25 \AA^{-1} the intensity in this region has been manually set to zero.

states is then given by

$$E_{\sigma\pm}(k) = E_0 - Dk^2 \pm \sqrt{\left(\frac{\Delta}{2} - Bk^2\right)^2 + (|V| + \sigma v_F \hbar k)^2}$$

The term $|V|$ represents the band bending across the film and together with $\sigma = \pm 1$ it produces a set of two Dirac cones with opposite helicities having their Dirac points separated in energy by $2|V|$. E_0 is now the center energy of the two Dirac points. The remaining parameters have the same meaning as in Eq. (1).

Fitting Eq. (2) to our data reproduces the observed band structure well, as seen in Fig. 1(d). Also in this case, only data points close to the Dirac points are used in the fit. The large V-shaped state observed in the simulated band structure (dashed line in Fig. 1(d)) corresponds to the Dirac cone at the interface between the TI and the substrate, which suggest that what we observe is indeed the interface state of the TI film. The fact that no such state is observed in the 8 QL ARPES data indicates that the thickness of this film is larger than the electron escape depth at this particular excitation energy and temperature.

In order to verify the interface nature of the observed feature in the 6 QL film we have performed photon energy dependent ARPES measurements at the I3 beamline at MAXlab [22]. A 6 QL film was measured at a photon energy of 10 eV displaying both the surface and the interface states. However, when increasing the photon energy to 22 eV only the surface state remained visible. The reduced intensity of the interface state in the photoelectron spectrum for higher excitation energy is consistent with the increased surface sensitivity of the ARPES technique in that particular photon energy range.

All together, the observed thickness and photon energy dependence of the states in the 6 QL film, combined with

	6 QL	6 QL	8 QL
Substrate doping	n -type	p -type	n -type
E_0 (eV)	-0.661	-0.580	-0.458
D (eV \AA^2)	-5.84	-2.23	-10.8
B (eV \AA^2)	0	0	0
Δ (eV)	0	0	0
V (eV)	0.135	0.144	-
v_F (10^5 m s^{-1}) (fit)	3.28	3.54	3.04
v_F (10^5 m s^{-1}) (actual)	5.8	4.8	5.9

TABLE I. Fitted parameters for the 6 QL films using Eq. (2) and for the 8 QL film using Eq. (1). Actual values for v_F along the $\bar{\Gamma}\text{-}\bar{K}$ direction, based on MDC peaks close to E_F , are also listed.

the agreement between the theoretical model and experimental data, support the notion that we directly observe the Dirac state located at the substrate interface. The interface state exhibits a similar Dirac-like dispersion as the surface state and is shifted towards higher binding energy as a result of band bending in the film.

In order to gain a qualitative understanding of the substrate effect, and hence the band bending in the film, we have studied 6 QL films grown on n -type (0.004 Ωcm) and p -type (0.0009 Ωcm) Si(111) substrates. Comparison reveals, interestingly, very little differences between the observed band structure of the films, see Fig. 2, although the bulk Fermi level (E_F) position in the two substrates are very different. In both cases the energy separation between the two Dirac points (ΔE_D) is roughly 0.3 eV.

The striking similarities between the 6 QL films on n -type and p -type substrates is a consequence of the Fermi level of the Si(111)-(7 \times 7) surface being pinned approximately 0.7 eV above the valence band maximum (E_V) due to a high density of states located in the band gap at the surface [23–25]. This pinning of E_F is independent of bulk doping and thus equivalent for both n -type and p -type substrates. Terminating the surface with 1 ML bismuth has little effect on the pinning level, reducing $E_F - E_V$ from 0.7 eV to approximately 0.65 eV [26].

From the measured value of ΔE_D we get the magnitude of the band bending across the film. The binding energy positions of the Dirac points, together with the known band gap of Bi_2Se_3 (0.35 eV [10, 27]), gives the Fermi level relative the conduction band minimum. Assuming an unchanged position of E_F at the substrate surface, alignment of the Fermi levels in the film and substrate results in conduction band offsets (ΔE_C) of 1.09 eV and 1.02 eV for the films on n -type and p -type substrate respectively. Here we have also assumed that the Dirac point is located in the center of the Bi_2Se_3 band gap. Figures 3(a) and 3(b) display the resulting band alignment for the $\text{Bi}_2\text{Se}_3/\text{Si}$ heterojunction. The upwards (downwards) band bending seen for the n -type (p -type) substrate is a result of the discussed pinning

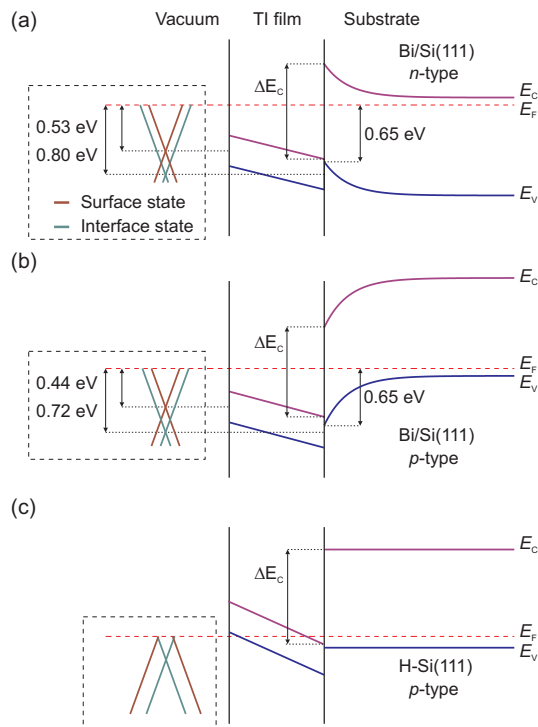


FIG. 3. (color online) (a) Band diagram for the Bi₂Se₃/Bi/*n*-Si system showing the conduction (E_C) and valence (E_V) bands in the thin film and substrate. The conduction band offset ΔE_C at the interface is 1.09 eV. The dashed horizontal line refers to the Fermi level, E_F . Vertical lines represent the vacuum/TI and TI/substrate interfaces respectively. A schematic drawing of the observed band structure for the surface and interface states with corresponding values for E_D is enclosed by the dashed rectangle. (b) Band diagram for the Bi₂Se₃/Bi/*p*-Si system for which $\Delta E_C=1.02$ eV. (c) Predicted band diagram for a *p*-doped Bi₂Se₃ thin film on a H-terminated Si(111) substrate.

of E_F at the surface. Therefore, the energy difference $E_F - E_V$ at the substrate side of the interface is the same in the two cases (0.65 eV). For simplicity, the band bending through the thin film is assumed to be linear. If we instead use the electron affinity rule [28] to determine the conduction band offset we obtain $\Delta E_C = 1.14$ eV. The electron affinities $\chi[\text{Si}(111)-(7 \times 7)] = 4.16$ eV [29] and $\chi[\text{Bi}_2\text{Se}_3] \sim 5.3$ eV have been used. The latter is an estimate based on the value of the work function of Bi₂Se₃ which is determined from the photoemission experiment. The similar values for ΔE_C obtained using the two approaches indicate that the sketched band alignment is qualitatively correct and that the pinned Fermi level position of the substrate is little influenced by the presence of the film. Also, the magnitude of ΔE_C at the Bi₂Se₃-Si interface is comparable to the band gap of silicon.

As seen from our results, using Si(111) substrates with very different doping levels does not influence the band bending through the Bi₂Se₃ thin films, as initially expected, due to the pinning of the Fermi level at the in-

terface. This seems to limit the possibilities of exploiting the bulk position of E_F in the substrate to modify the electronic configuration of TI thin films. However, this problem might be overcome by instead using a H-terminated substrate. At the H-Si(111) surface the pinning of E_F is removed [30, 31] and the unpinned position is determined by the Fermi level in the bulk. Tuning the position of E_F in the substrate by bulk doping can then be used to manipulate the band bending across the film.

Since the conduction band offset ΔE_C at the interface is fixed, tuning of the chemical potential in the film by Ca or Mg-doping [32, 33] is expected to shift the surface Dirac point towards lower binding energy. We propose the idea of using a heavily *p*-doped H-Si(111) substrate combined with a *p*-doped Bi₂Se₃ film to obtain the band alignment presented in Fig. 3(c). If the film is sufficiently doped, the chemical potential at the surface can be placed below the Dirac point which would result in a hole-like surface state and electron-like interface state as shown in Fig. 3(c). This system could then host bound electron-hole pairs, or excitons, and possibly permit the observation of a topological exciton condensate (TEC) as suggested in Ref. [34].

The work presented in this article establishes experimentally the existence of interface states at the interface between a trivial insulator and a topological insulator. Similar to the surface state on Bi₂Se₃ the interface state exhibits a Dirac-like linear dispersion. The band bending through the film, generated by the substrate, shifts the Dirac point of the interface state in energy relative to the surface state. We predict that H-termination of the Si(111) substrate will allow the band bending across the film to be manipulated by changing the doping level and carrier type of the substrate. Our work also shows that the combination of low-temperature and low-photon-energy ARPES permits direct studies of buried interfaces in these materials, something which opens up for further studies on, for example, interfaces in *p-n* TI junctions and TI-heterojunctions.

This work was made possible through support from the Knut and Alice Wallenberg Foundation and the Swedish Research Council.

-
- [1] L. Fu, C. L. Kane, and E. J. Mele, Phys. Rev. Lett. **98**, 106803 (2007).
 - [2] J. E. Moore and L. Balents, Phys. Rev. B **75**, 121306(R) (2007).
 - [3] L. Fu and C. L. Kane, Phys. Rev. B **76**, 045302 (2007).
 - [4] O. V. Yazyev, J. E. Moore, and S. G. Louie, Phys. Rev. Lett. **105**, 266806 (2010).
 - [5] H. Steinberg, J.-B. Laloë, V. Fatemi, J. S. Moodera, and P. Jarillo-Herrero, Phys. Rev. B **84**, 233101 (2011).
 - [6] X.-L. Qi, R. Li, J. Zang, and S.-C. Zhang, Science **323**, 1184 (2009).

- [7] L. Fu and C. L. Kane, *Phys. Rev. Lett.* **100**, 096407 (2008).
- [8] R. Li, J. Wang, X.-L. Qi, and S.-C. Zhang, *Nature Phys.* **6**, 284 (2010).
- [9] H. Zhang, C.-X. Liu, X.-L. Qi, X. Dai, Z. Fang, and S.-C. Zhang, *Nature Phys.* **5**, 438 (2009).
- [10] Y. Xia, D. Qian, D. Hsieh, L. Wray, A. Pal, H. Lin, A. Bansil, D. Grauer, Y. S. Hor, R. J. Cava, and M. Z. Hasan, *Nature Phys.* **5**, 398 (2009).
- [11] Z.-H. Pan, E. Vescovo, A. V. Fedorov, D. Gardner, Y. S. Lee, S. Chu, G. D. Gu, and T. Valla, *Phys. Rev. Lett.* **106**, 257004 (2011).
- [12] C. Jozwiak, Y. L. Chen, A. V. Fedorov, J. G. Analytis, C. R. Rotundu, A. K. Schmid, J. D. Denlinger, Y.-D. Chuang, D.-H. Lee, I. R. Fisher, R. J. Birgeneau, Z.-X. Shen, Z. Hussain, and A. Lanzara, *Phys. Rev. B* **84**, 165113 (2011).
- [13] G. Zhang, H. Qin, J. Teng, J. Guo, Q. Guo, X. Dai, Z. Fang, and K. Wu, *Appl. Phys. Lett.* **95**, 053114 (2009).
- [14] J.-H. Song, H. Jin, and A. J. Freeman, *Phys. Rev. Lett.* **105**, 096403 (2010).
- [15] Y. Zhang, K. He, C.-Z. Chang, C.-L. Song, L.-L. Wang, X. Chen, J.-F. Jia, Z. Fang, X. Dai, W.-Y. Shan, S.-Q. Shen, Q. Niu, X.-L. Qi, S.-C. Zhang, X.-C. Ma, and Q.-K. Xue, *Nature Phys.* **6**, 584 (2010).
- [16] Y. Sakamoto, T. Hirahara, H. Miyazaki, S. I. Kimura, and S. Hasegawa, *Phys. Rev. B* **81**, 165432 (2010).
- [17] W.-Y. Shan, H.-Z. Lu, and S.-Q. Shen, *New J. Phys.* **12**, 043048 (2010).
- [18] M. P. Seah and W. A. Dench, *Surf. Interface Anal.* **1**, 2 (1979).
- [19] M. H. Berntsen, O. Götzberg, and O. Tjernberg, *Rev. Sci. Instrum.* **82**, 095113 (2011).
- [20] K. Kuroda, M. Arita, K. Miyamoto, M. Ye, J. Jiang, A. Kimura, E. E. Krasovskii, E. V. Chulkov, H. Iwasawa, T. Okuda, K. Shimada, Y. Ueda, H. Namatame, and M. Taniguchi, *Phys. Rev. Lett.* **105**, 076802 (2010).
- [21] H.-Z. Lu, W.-Y. Shan, W. Yao, Q. Niu, and S.-Q. Shen, *Phys. Rev. B* **81**, 115407 (2010).
- [22] M. H. Berntsen, P. Palmgren, M. Leandersson, A. Hahlin, J. Åhlund, B. Wannberg, M. Månsson, and O. Tjernberg, *Rev. Sci. Instrum.* **81**, 035104 (2010).
- [23] F. J. Himpsel, D. E. Eastman, P. Heimann, B. Reihl, C. W. White, and D. M. Zehner, *Phys. Rev. B* **24**, 1120 (1981).
- [24] F. J. Himpsel, G. Hollinger, and R. A. Pollak, *Phys. Rev. B* **28**, 7014 (1983).
- [25] J. M. Nicholls and B. Reihl, *Phys. Rev. B* **36**, 8071 (1987).
- [26] K. Hricovini, G. Le Lay, A. Kahn, A. Taleb-Ibrahimi, J. E. Bonnet, L. Lassabatère, and M. Dumas, *Surf. Sci.* **252**, 424 (1991).
- [27] J. Black, E. M. Conwell, L. Seigle, and C. W. Spencer, *J. Phys. Chem. Solids* **2**, 240 (1957).
- [28] R. L. Anderson, *Solid-State Electron.* **5**, 341 (1962).
- [29] G. Hollinger and F. J. Himpsel, *J. Vac. Sci. Technol. A* **1**, 640 (1983).
- [30] C. J. Karlsson, E. Landemark, L. S. O. Johansson, U. O. Karlsson, and R. I. G. Uhrberg, *Phys. Rev. B* **41**, 1521 (1990).
- [31] R. Hunger, C. Pettenkofer, and R. Scheer, *J. Appl. Phys.* **91**, 6560 (2002).
- [32] D. Hsieh, Y. Xia, D. Qian, L. Wray, J. H. Dil, F. Meier, J. Osterwalder, L. Patthey, J. G. Checkelsky, N. P. Ong, A. V. Fedorov, H. Lin, A. Bansil, D. Grauer, Y. S. Hor, R. J. Cava, and M. Z. Hasan, *Nature (London)* **460**, 1101 (2009).
- [33] Y. L. Chen, J.-H. Chu, J. G. Analytis, Z. K. Liu, K. Igarashi, H.-H. Kuo, X. L. Qi, S. K. Mo, R. G. Moore, D. H. Lu, M. Hashimoto, T. Sasagawa, S. C. Zhang, I. R. Fisher, Z. Hussain, and Z. X. Shen, *Science* **329**, 659 (2010).
- [34] B. Seradjeh, J. E. Moore, and M. Franz, *Phys. Rev. Lett.* **103**, 066402 (2009).